Development of a liquid lithium thin film for use as a heavy ion beam stripper

Yoichi Momozaki[a*], Jerry Nolen[b†], Claude Reed[a], Vincent Novick[a] and James Specht[b]

[a] *Argonne National Laboratory, Nuclear Engineering Division, 9700 South Cass Avenue, Argonne, Illinois 60439, U.S.A.*
[b] *Argonne National Laboratory, Physics Division, 9700 South Cass Avenue, Argonne, Illinois 60439, U.S.A.*
E-mail: momo@anl.gov

ABSTRACT: A series of experiments was performed to investigate the feasibility of a liquid lithium thin film for a stripper in a high power heavy ion linac. Various preliminary experiments using simulants were first conducted to determine the film formation scheme, to investigate the film stability, and to obtain the design parameters for a liquid lithium thin film system. Based on the results from these preliminary studies, a prototypical, high pressure liquid lithium system was constructed to demonstrate liquid lithium thin film formation. This system was capable of driving liquid lithium at <~300 °C and up to 13.9 MPa (2000 psia) through a nozzle opening as large as 1 mm (40 mil) in diameter. This drive pressure corresponds to a Li velocity of >200 m/s. A thin lithium film 9 mm in width at velocity of ~58 m/s was produced. Its thickness was estimated to be roughly ≤~13 μm. High vacuum was maintained in the area of the film. This type of liquid metal thin film may also be used in other high power beam applications such as for intense X-ray sources.

KEYWORDS: Instrumentation for heavy-ion accelerators (heavy ion beams; stripping foils; liquid lithium technology).

* Corresponding author.
† Corresponding author.

Contents

1. Introduction

The proposed Advanced Exotic Beam Laboratory (AEBL) will produce various high-power, unstable isotope beams [1]. A high-power ion beam will be generated in a driver linac and delivered to targets for isotope production. One of the challenges is to develop a charge stripper in the driver linac for efficient uranium beam acceleration. This type of stripper is also potentially useful for high-power heavy ion beam facilities, such as the Radioisotope Beam Facility (RIBF) at Riken in Japan. This stripper needs to withstand large power input from intense ion bombardment. A liquid lithium stripper is considered a primary candidate for use in the driver linac (see Figure 1), because liquid lithium has good nuclear physics and thermal properties to strip electrons from heavy (uranium) ion beams at low energies and to remove very high heat input while maintaining vapor pressure sufficiently low. In addition, recently, the feasibility of using liquid lithium as a windowless liquid target in an isotope beam facility was experimentally investigated at Argonne National Laboratory (ANL) [2] and results showed an excellent thermal handling capability of the liquid target concept in high power accelerator applications. Also shown was good compatibility of a liquid lithium system with accelerator environments. These results are very promising and support the development of a liquid lithium stripper.

Although the use of a liquid lithium thin film as an electron stripper for heavy ion beams has potential advantages, there are technical uncertainties that need to be investigated. For example, preliminary analysis from the viewpoint of nuclear physics indicates that the optimum thickness of such a liquid lithium first stripper could be on the order of 10-20 micrometers, for uranium beam energies in the 10-20 MeV/u range. The necessary film thicknesses and charge state distributions are obtained from a combination of systematics from measurements at several heavy ion facilities and simulations by programs such as ETACHA [3] and GLOBAL [4] , and data fit with parameters [5]. To provide consistent stripping characteristics, the shape, especially the thickness, of the film must be kept constant and stable for a long time. (> ~hours)

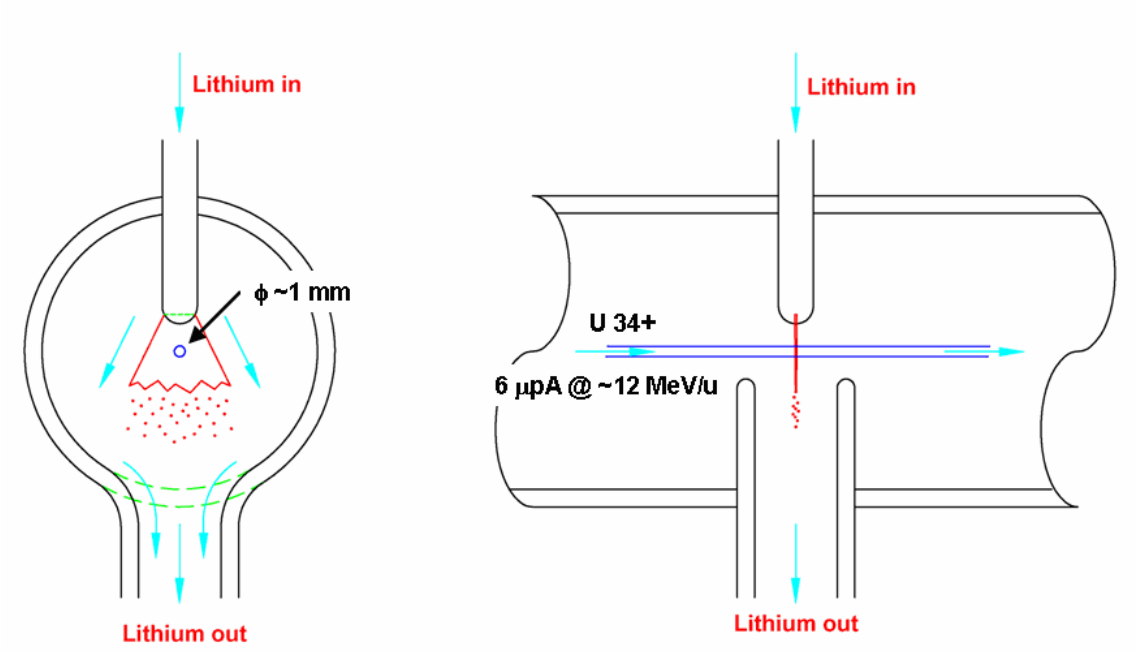

Figure 1. Conceptual diagram of liquid lithium thin film stripper for uranium beam with some typical design parameters indicated.

The width and the length of the film need to be larger than the size of an ion beam whose diameter is typically ~1 mm or less. Also, to avoid excessive vaporization of the liquid lithium, the mass flow rate of the jet must be high enough to remove the thermal energy deposited in the film from the beam without a significant temperature rise. To the best of our knowledge, producing a very thin, stable film jet with a high flow rate using a liquid metal in a vacuum environment has not been previously demonstrated. However, a non-metal liquid jet issuing from a nozzle into non-vacuum environments in general has been investigated for more than a century. It has been shown that a liquid jet emanating from a nozzle is inherently unstable, meaning that any liquid jets will eventually break up, as they evolve either in time or in space. Any slight disturbances in the jet are spontaneously amplified in space and time depending on conditions, therefore the jet eventually breaks up into small droplets, which is caused by capillary pinching [6]. A disturbance propagating both in space as well as in time is called *absolute instability*. This occurs when the surface tension forces in the fluid dominate over the inertial forces in the fluid of the jet. This is the case for small fluid velocity. Here the liquid does not form a temporally stable jet and forms droplets as soon as it exits from the nozzle in absolute instability mode. As the jet velocity increases, the inertia becomes dominant and the instability shifts to the *convective instability* mode, in which a disturbance propagates and grows only in the downstream (spatial) direction. Because the disturbance does not grow in time, a continuous jet is formed from the nozzle and it extends to the point, at which the spatially growing disturbance in the jet eventually breaks up the jet. This type of jet in the convective instability mode is therefore considered temporally stable but spatially unstable. When the amplitude of the disturbance imposed on the jet grows large enough, capillary pinching due to

the surface tension of the fluid causes breakup of the jet. These instability phenomena can place constraints on the stable operation range of a liquid lithium thin film stripper.

Since jet instability phenomena in a vacuum involve only the surface tension, viscous force, and inertial force, they are expected to be a function of these three parameters and characteristics of the applied disturbances. Combinations of two dimensionless parameters, the Reynolds number, *Re* (= inertial force/viscous force) and the Weber number, *We* (= inertial force/surface tension force), could be used to represent effects of these three parameters. The range of temporally stable jet formation may be represented in a *Re* and *We* parameter space. When a temporally stable jet is formed, the spatial length of the jet strongly depends on the amplitude of the initial disturbance and the size of the liquid jet, in other words, it depends on the physical dimensions of the nozzle, the surface finish of the nozzle interior, any externally induced pressure fluctuations in the fluid, and any mechanical vibrations, etc. Especially, the quantities such as surface finish, pressure fluctuation, and vibration in a real system are extremely hard to determine. Therefore, it is not reasonable to expect to theoretically estimate the physical dimensions of a jet with a high degree of accuracy, making an experimental measurement the only practical method to investigate the feasibility of a liquid lithium thin film stripper [7].

The main objective of the present work is to demonstrate the formation of a temporally stable liquid lithium thin film jet in vacuum environment, simulating a stripper useful for high intensity heavy ions such as uranium in the energy range of ~10-20 MeV/u. Because of the extreme technical difficulty of conducting a variety of developmental investigations using liquid lithium, it was decided to use Li simulants as much as possible. Since jet instability phenomena in a vacuum may be represented by *Re* and *We*, we assume that experiments using Li simulants could be a reasonable tool to predict hydrodynamics of Li as long as both *Re* and *We* are kept the same as those expected for a liquid lithium case. The temporal stability diagram as a function of *Re* and *We* was experimentally developed using simulants for the specific film production scheme. This stability diagram is expected to provide the range of design parameters that are potentially capable of producing a temporally stable liquid lithium film whose spatially smooth length is reasonably long to be used as a stripper. Therefore, the present work is divided threefold: (1) experimentally develop the liquid thin film formation scheme, (2) experimentally develop the film temporal stability diagram for the selected film formation scheme using Li simulants and determine design parameters for a Li system for thin liquid lithium film formation, and (3) experimentally demonstrate the thin film liquid lithium jet and confirm that the dimensions of the film are in a useful range to be used as a stripper.

The first section of this paper describes preliminary experiments using simulant working fluids. In these preliminary experiments, different thin film formation schemes were investigated and the most suitable scheme for producing a liquid lithium thin film was determined. Also described in this section is the experimental development of the *Re* vs. *We* stability diagram. The design parameters were determined, and the design guidelines were developed, for a Li thin film system based on the results obtained in these experiments. The second section describes the experimental setup, procedures, and results, explaining experiments demonstrating the formation of a liquid lithium thin film jet. A prototypical, high pressure liquid lithium system to demonstrate liquid lithium thin film formation was constructed. The behavior of the liquid lithium thin film jet was visually observed to confirm temporally stable jet formation. The drive pressure, temperatures at various locations, and the

background pressure were also monitored. Based on those visual observations and drive pressures, the velocity, width, and length of the thin film jet were estimated.

2. Preliminary experiments using simulant working fluids

2.1 Development of the liquid thin film formation scheme

The most straight forward method to produce a liquid film would be a direct method, using a slit nozzle whose dimensions match the required film dimensions. For the desired uranium beam stripper, however, since the film thickness required from physics considerations is only of the order of 10-20 micrometers and the width of the film must be of the order of several millimeters, it was considered to be extremely difficult to fabricate such a high aspect-ratio nozzle with a very narrow opening. Also, such a narrow opening is expected to be prone to plugging by particulates of foreign material and/or lithium compounds during operation and was not considered suitable. Other proposed methods produce a film indirectly. In one proposed method, liquid issues from a round nozzle, forming a round jet, which subsequently impacts on a deflector, on which the round jet transforms into a thin film. In this method, use of a high aspect ratio nozzle is not necessary and the size of the nozzle opening could be much larger than the thickness of the thin film, making the nozzle less prone to plugging. Preliminary experiments showed that a nice thin water jet can be produced using a round nozzle and a metal deflector.

In conclusion, the indirect method using a stationary deflector, in which a round jet from a round nozzle impacts on a deflector on which the round jet is transformed into a thin film, appears to be the best film forming scheme.

2.2 Experimental development of the film stability diagram using Li simulants

After analyzing properties of various potential Li simulants, including liquid metals, water seemed to be the best candidate. Also, 3M Corporation's FC-3283 was found to have very unique characteristics, exhibiting differences in physical properties used to calculate *We* and *Re* between FC-3283 and water that are similar to those between water and lithium (see Table 1). This implies that if insignificant differences between FC-3283 and water film behaviors are observed throughout a certain Re and We parameter space, then essentially the same behavior would be expected of the lithium film in that same Re and We parameter space. In addition, inert and non-hazardous characteristics of water and FC-3283 significantly reduce complexity, difficulty, and cost of performing a variety of developmental experiments. Using *Re*-*We* scaling, a Li film at 10 μm thick, 473 K, and 50 m/s, for example, is equivalent to a water film at 58 μm thick, 303 K, and 6.4 m/s and to an FC-3283 film at 420 μm thick, 303 K, and 0.83 m/s. For all these 3 films, $Re = 450$, $We = 33$.

Prior to designing and fabricating a Li thin film stripper system, several series of experiments using Li simulants were performed to investigate the film behavior and to determine the range of stable jet formation. Changing the drive pressure changed the jet velocity as well as the thickness of the film. As an attempt to independently vary the film thickness, nozzle diameter was also changed in the experiments. It was experimentally found that the nozzle diameter of ~0.5 mm may be the largest size to form a nice, smooth film. Tests with the nozzle diameters ≥ 1.0 mm produced films with large ripples, which is not suitable to be used as a stripper.

Table 1. Various physical properties of Lithium, Water, and FC-3283 and ratios of FC-3283/Water and Water/Lithium.

	Lithium	Water	FC-3283
Temperature [K]	473.15	298.15	R.T.
Density [kg/m^3]	515.0	996.5	1820.0
Surface tension [N/m]	0.3921	0.0719	0.0160
Viscosity [Pa-s]	5.72E-04	9.11E-04	1.40E-03

	FC-3283/Water		Water/Lithium
Temperature [K]	R.T./298.15		298.15/473.15
Density ratio	1.83		1.94
Surface tension ratio	0.222		0.183
Viscosity ratio	1.54		1.59

The stability diagrams presented as *Re* vs. *We* numbers for water and FC-3283 seemed to be very similar, indicating such diagrams may be considered universal (Figure 2). The effects of surrounding air on instability were confirmed to be negligible for water due to their low flow velocities near the instability threshold.

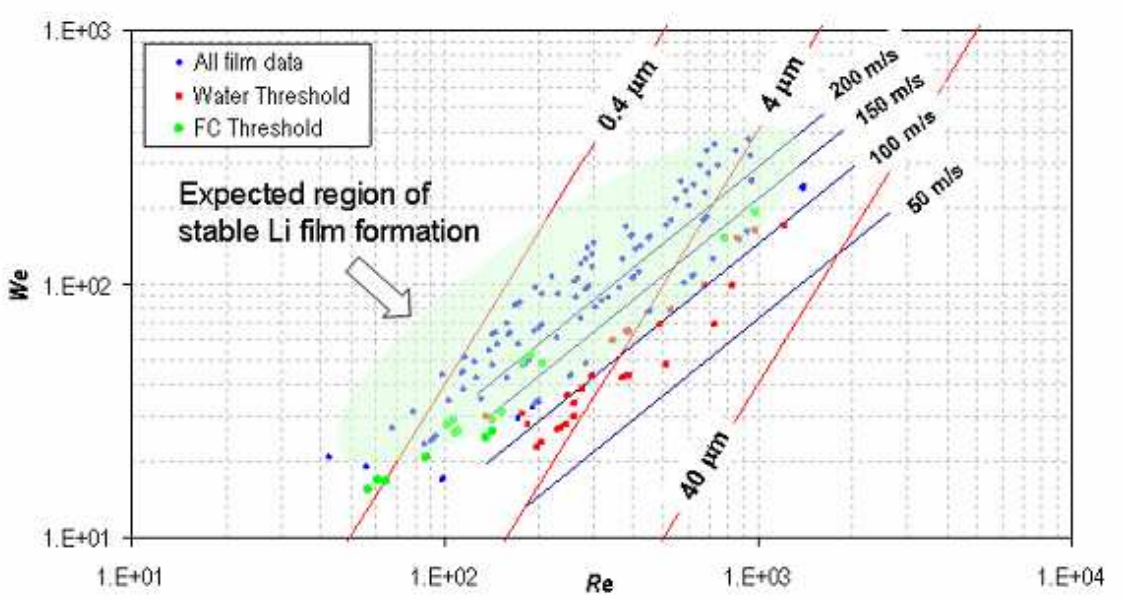

Figure 2. Experimentally developed stability diagram. The inserted labels are scales to the parameters of lithium.

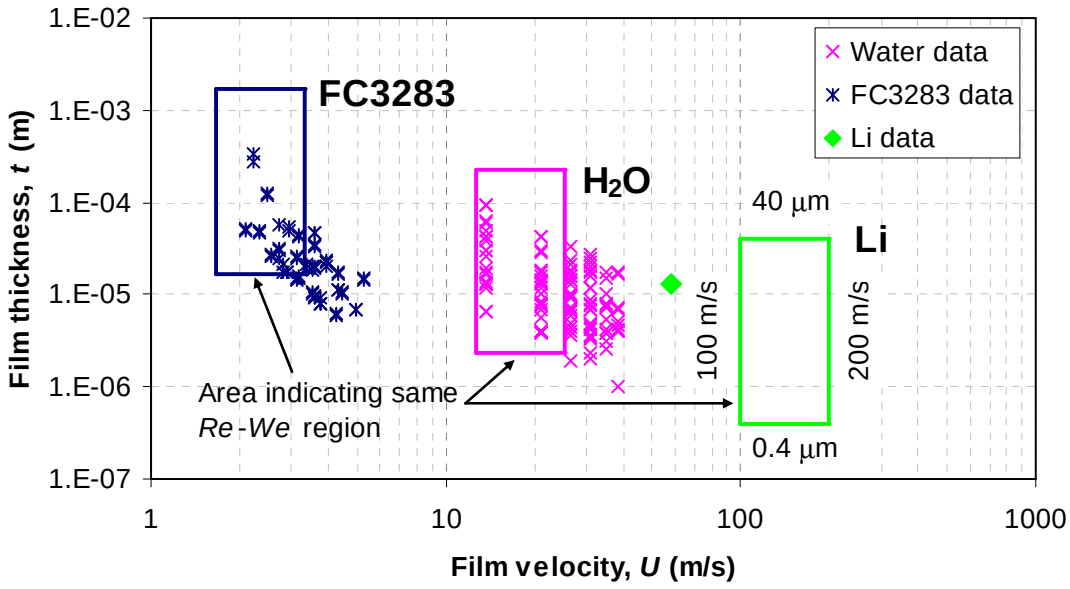

Figure 3. Thickness of various demonstrated thin films as a function of film velocity.

Figure 2 shows that both water and FC-3283 threshold data (velocity below which no film data points in the figure, form a single, relatively narrow band in *Re*-*We* space, indicating that formation was observed, presumably due to absolute instability), represented by green and red the temporal stability boundary above which formation of films with finite length is expected (green shaded region in Figure 2) may exist and that this temporal stability boundary may be fairly universal. Note that water and FC-3283 films with conditions below this narrow band, representing the temporal stability boundary, fall in the absolute instability regime and temporally stable film formation was not observed. Values for velocity and film thickness in Figure 2 are for Li. This figure suggests that a Li film of <~10 μm thickness at >~100 m/s would be stable. The same data presented in Figure 2 are also plotted in the film velocity-film thickness space (Figure 3). This figure shows that for the same set of *Re* and *We*, the differences in physical parameters for FC-3283 and water are approximately the same as those for water and lithium. For the same *Re* and *We*, no apparent differences in film behavior was observed between FC-3283 and water films, suggesting insignificant difference in film behavior between water and Li films would be expected.

2.3 Conclusions of preliminary experiments with simulants

The films of different fluids appear to behave in a similar manner when their *Re* and *We* are kept the same and if the shear stress with surrounding media can be neglected. Although larger nozzle size is better to avoid potential plugging, it was experimentally found that the nozzle diameter of ~0.5 mm may be the largest size to form a nice film. Tests with the nozzle diameters ≥1.0 mm produced films with large ripples, thus the nozzles with the diameter ≥1.0 mm are not considered appropriate. Also, to form a temporally stable Li thin film, a Li jet needs to be issued at > ~100–150 m/s (see Figure 2), whose corresponding drive pressure is 3–6 MPa. Other findings are that the angle of incidence should be between 30–45 degrees and the relative position of the nozzle with respect to the deflector must be adjustable to an accuracy of ~0.1mm

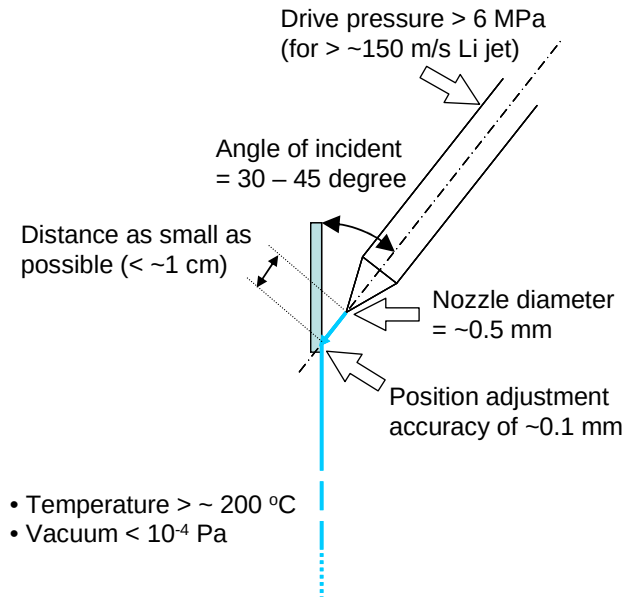

Figure 4. Summary of critical design parameters.

(Figure 4). One additional finding was that the water jet near the exit of the nozzle sometimes did not initially look smooth and straight. While increasing the drive pressure further, the jet suddenly changed into a nice, smooth jet at drive pressures as high as 2-3 times the pressure for a good film formation. As soon as the jet became smooth, the drive pressure could be reduced to the desired pressure and the jet usually stayed smooth at reduced pressures. We are speculating that the opening of the nozzle was wetted, and the jet attached to the side wall of the orifice at the moment of jet initiation (Figure 5). The jet, then, may have been dragged toward that wetted part of the side wall in an uncontrolled manner, disturbing the quality of the jet. However, when the inertia of the jet became high enough (as the drive pressure was increased) the jet finally separated at the edge of the entrance of the orifice and did not touch the side wall of the orifice or the nozzle, forming a well defined, smooth jet.

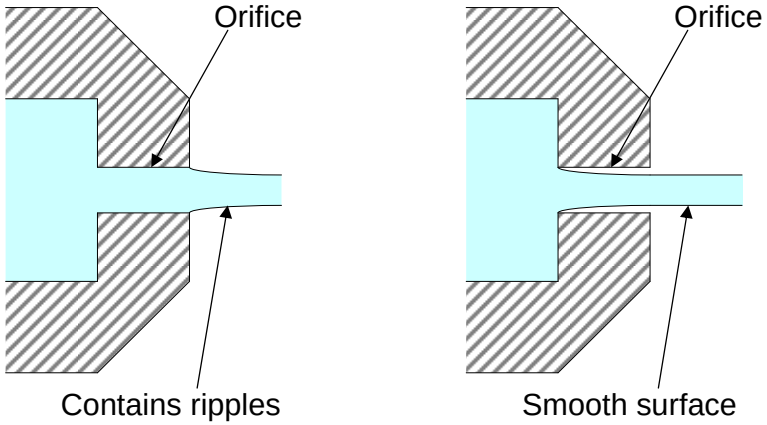

Figure 5. Suggested mechanism of forming jet with ripples.

3. Experimental setup and procedure for lithium experiments

A prototypical, high pressure liquid lithium system was constructed based on the findings in the preliminary study described in the previous section. Since a need of the relatively high drive pressure was expected, the system employed “once-through” concept, in which the high speed lithium jet is driven by high pressure compressed gas. The lithium is stored in a pressure vessel that pressurizes the lithium to the desired drive pressure by the compressed argon. This setup allowed increasing the drive pressure significantly higher than a “continuously-circulating” system with a Li pump can. Some of the drawbacks include the limited operation time, requiring relatively large lithium inventory, and technical difficulties associated with use of high

pressure. Based on this experiment, exact requirements for a Li pump for such a "continuously-circulating" system can be determined. It must be noted that for a practical stripper system, the continuously circulating system is necessary.

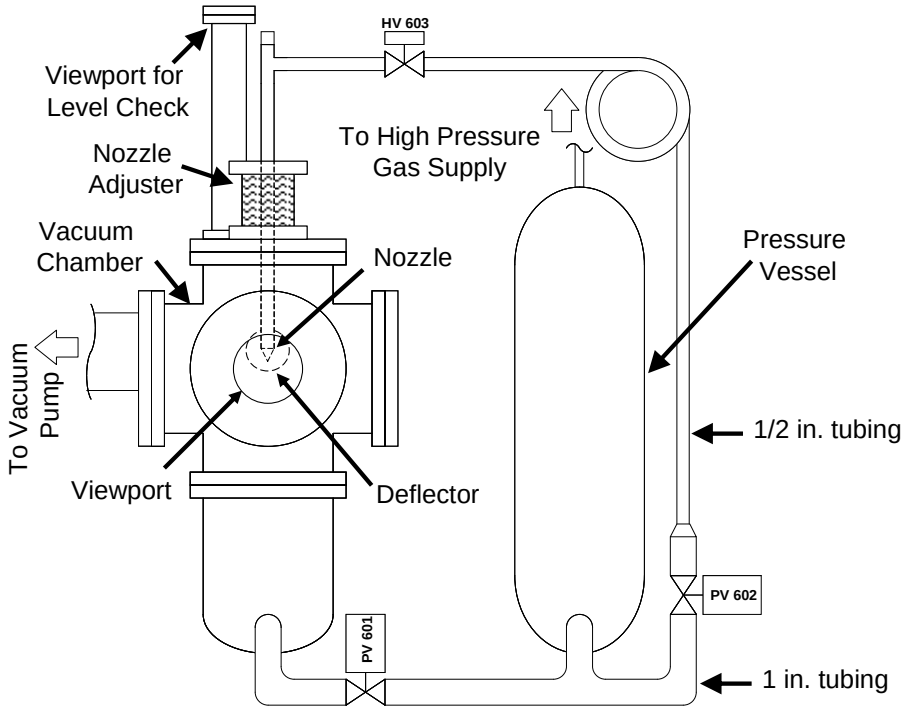

Figure 6. Schematic of Li system.

The whole system consisted of a lithium system, a vacuum system, a high pressure gas system, and a low pressure gas system. The lithium system and vacuum system were installed in a containment room made from stainless steel to confine lithium in case of leak. The containment room was equipped with a scrubber that removes any particulates of lithium compounds from combustion gases in case of fire. The lithium system was also enclosed in a secondary containment made from stainless steel sheet metal. This secondary containment also served as a thermal barrier to minimize parasitic heat losses from the lithium system during operation. The containment was covered with heat resistant cloth that provided further thermal insulation and that also prevented burning from accidental contact. The lithium system was sub-divided into the following components; a vacuum chamber, in which a liquid lithium thin film was formed, a pressure vessel, in which liquid lithium was stored and pressurized up to 13.9 MPa (=2000 psi), and lithium lines that connect the chamber and vessel (see Figure 6). The inventory of Li in the system was 11.5 kg (~22.3 liters) of which the maximum usable quantity was ~16.7 liters. The major components of the system were fabricated from stainless steel for compatibility with liquid lithium. Connections that were in contact with liquid lithium were welded as much as possible. However, some connections used metal-to-metal seals to facilitate component replacement. Conflat flanges with annealed iron gaskets used in place of the standard copper gaskets are used for connections that were exposed to high vacuum ($<\sim10^{-4}$ Pa) and low pressure (~0.1 MPa). Cajon VCR connectors with stainless steel gaskets were used for connections that were exposed to high vacuum ($<\sim10^{-4}$ Pa) and high pressure (>10 MPa).

No other types of connections were used in the lithium line. The core of the nozzle assembly consisted of an A.M. Gatti's* Hi-cohesive nozzle adaptor (P/N 3210) and specially ordered High-performance waterjet orifice assembly [P/N 3024 with a 0.5 mm (20 mil) round opening], which were all stainless steel. The original waterjet orifice assembly consists of a stainless steel nozzle body and a sapphire orifice. However, a compatibility test at ANL showed that sapphire is not compatible with molten lithium. Therefore, this all stainless steel orifice assembly was specially ordered. Both the original assembly with a sapphire orifice and the all stainless steel assembly were tested using water. The quality of the film from the all stainless steel assembly was slightly inferior to that from the original assembly at only very small jet velocity near the instability threshold. This system could safely drive liquid lithium at up to 13.9 MPa (2000 psia) through a nozzle with an opening as large as 1 mm (40 mil) in diameter into a vacuum chamber.

The nozzle assembly was mechanically-loosely mounted to the top of the vacuum chamber via the nozzle adjuster that consists of 4 springs (see Figure 6). Compressing and/or decompressing each spring allowed adjusting the flow direction and distance between the nozzle tip and the deflector. The coiled section of the 1/2 inch tubing between the nozzle assembly and the pressure vessel (see Figure 6) provided sufficient flexibility to the Li line for nozzle adjustment.

The deflector was a round plate whose surface was carefully machined to provide a smooth and highly polished plane for a Li round jet to impact and to transform into a thin film. The outer edge of the deflector was machined to provide sharp, right-angle edge. The deflector was mounted at the end of a hollow tube, which was inserted in the vacuum chamber through a Swagelok Ultra-Torr vacuum fitting, allowing linear and rotational motion of the tube with respect to the vacuum chamber. A type-K thermocouple (TC) was inserted in the tube to monitor the temperature of the deflector. The deflector had 3 sectors with slightly different radii, providing additional ability to adjust the distance between the impaction point and edge as well as the angle of incidence between the jet and the deflector, by rotating the deflector.

A Cooke Vacuum Products DP 2-325 air cooled diffusion pump, using Santovac 5, maintained the system under vacuum of low 10^{-7} Torr range at room temperature and low 10^{-6} Torr range during operation. The high pressure gas system provided high purity (99.998 %), high pressure Ar gas at up to 13.9 MPa (2000 psig) to the pressure vessel for driving liquid lithium out from the nozzle. The low pressure gas system provided an ultra high purity (>99.999 %) and low pressure (<3 psig) Ar gas as a cover gas and driving pressure to transfer liquid lithium from the collection chamber to the pressure vessel after each run.

A multiple zone heating system using ceramic band heaters controlled the system temperature and temperature distribution and minimized hot/cold spots which could result from significant differences in metal mass from component to component.

As a precaution against plugging at the nozzle, extra care was taken to keep lithium as clean as possible in the system. The system was baked for a few days at up to 300 °C under vacuum for outgassing prior to loading Li. At the end of the outgassing, the pressure in the system reached ~1×10^{-6} Torr range at 300 °C. Lithium rods were carefully loaded under an Ar environment using a Glove Bag from Gras-Col.

---

*TEL:1-800-882-0105,
524 Tindall Avenue, Trenton, NJ 08610, USA

A typical experiment started by heating the system to around 220 °C. After all temperatures along the system were stabilized and the nozzle and deflector temperatures exceeded the melting point of Li (181 °C), the pressure vessel was pressurized with Ar gas to a desired value. Then the valve 602 was opened to initiate a Li jet. The drive pressure was usually set above ~700 kPa (~100 psia). The formation of the jet was confirmed visually through the viewport. After the jet flow was established, the position of the nozzle assembly was finely adjusted to optimize the location of the impaction point respect to the deflector edge to form the best looking film. The temperatures and pressures were recorded at a set interval. A digital camcorder recorded visual images of the Li film from the viewport during experiments. These recorded visual images as well as temperatures and pressures form the basis of the present work.

4. Results

A few experiments for demonstrating formation of a thin liquid lithium film were performed at various driving pressures up to ~4 MPa (~600 psia). Continuous operation of the system is not possible, since the system employed the once-through concept to achieve very high Li jet velocity, however, due to the relatively small flow rate of Li and large Li inventory, the duration of a run at ~700 kPa (~100 psia) was as long as ~40 minutes. For example, Figure 7 shows the history of drive pressure for test 09/26/2005 #2.

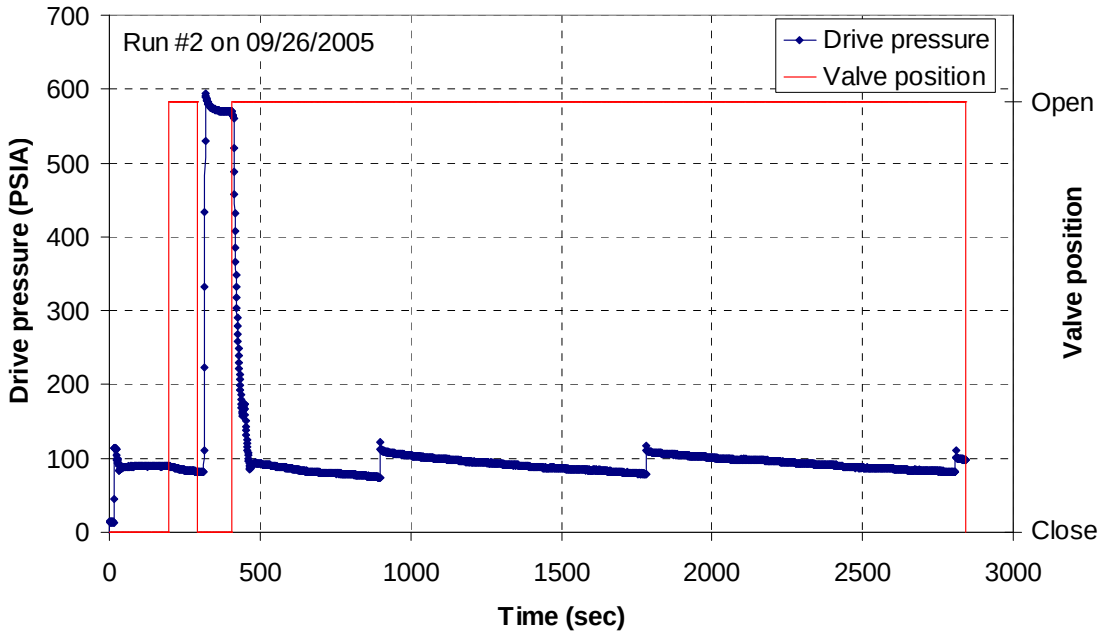

Figure 7. Drive pressure during Test 09/26/2005 #2.

Figure 8 shows various temperatures during test 09/26/2005 #2. Since the nozzle assembly did not have a heater directly attached to it, its temperature was dictated by conduction through the nozzle alignment assembly and radiation from the vacuum chamber, creating the temperature difference observed in this figure before 198 sec. As soon as liquid Li started to flow, it equalized the temperature distribution along the Li line including the nozzle assembly.

Heat transfer to the deflector was the same way. However, only a small portion of the deflector came into contact with liquid Li and the TC was located some distance away from the deflector itself and therefore the temperature reading indicated a somewhat lower temperature.

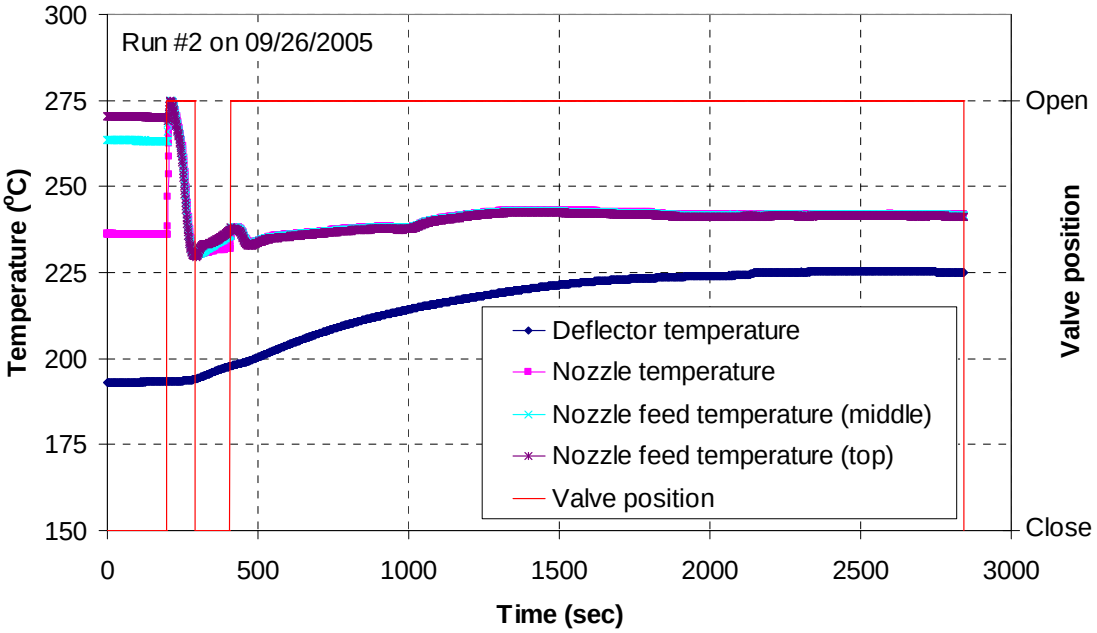

Figure 8. Temperatures during Test 09/26/2005 #2.

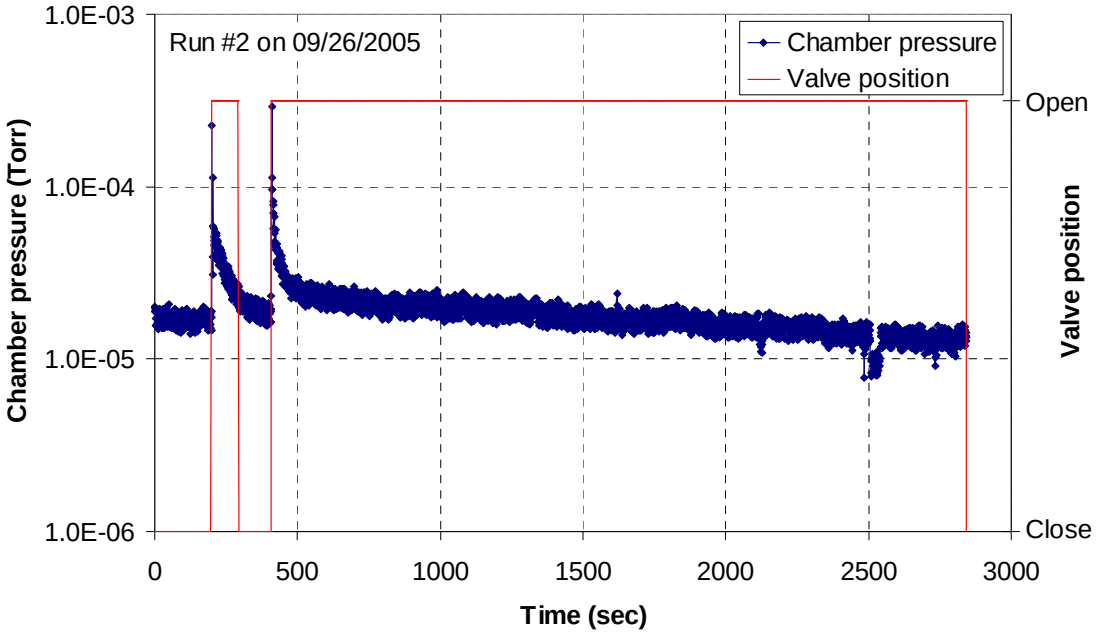

Figure 9. Chamber pressure during Test 09/26/2005 #2.

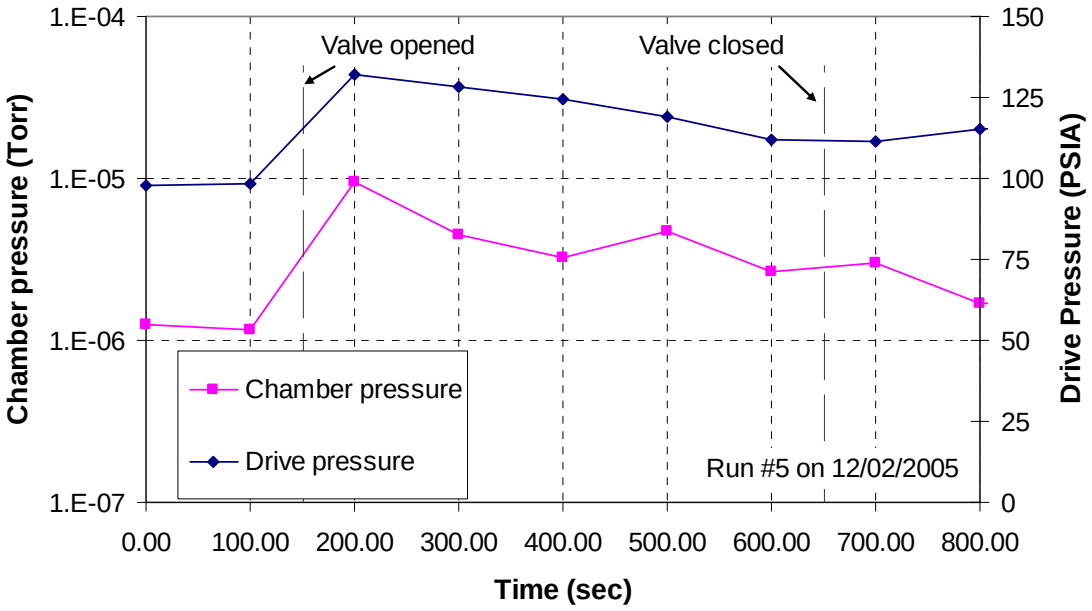

Figure 10. Drive and chamber pressures during Run 5.

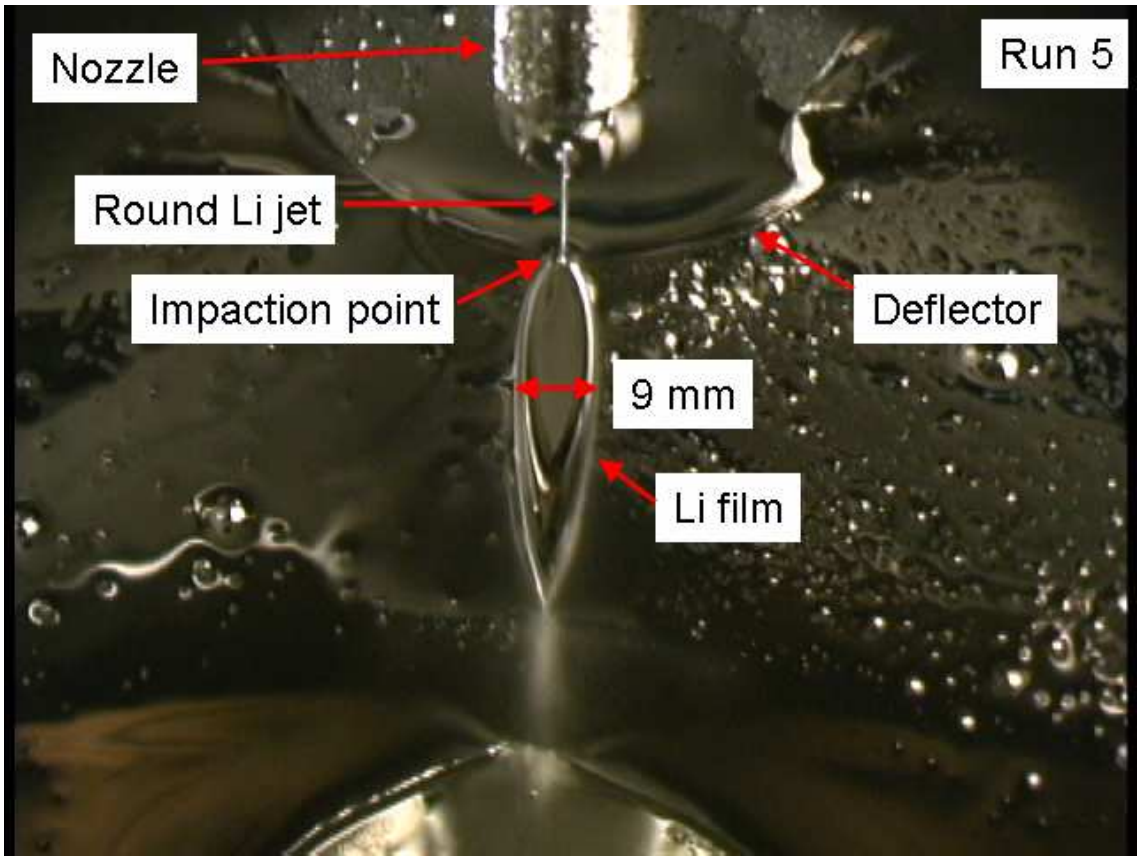

Figure 11. Photograph of a liquid lithium thin film.

Figure 9 shows the chamber pressure during the 09/26/2005 #2 test. Although the pressure momentarily went up to $>10^{-4}$ Torr right after valve 602 was opened, it quickly came down to low 10^{-5} Torr range. However, a later experiment on 12/02/2005 after about 2 months of continuous outgassing at room temperature shown in Figure 10, indicated lower chamber pressure in the 10^{-6} Torr range during the test, suggesting Li vapor was not a major contributor to the chamber pressure. In this experiment, observed Li temperature was ~250 °C, at which Li saturated vapor pressure is 4.5×10^{-6} Pa (3.4×10^{-8} Torr).

Figure 11 shows a photograph of a liquid Li thin film obtained on 12/02/2005. The drive pressure was ~860 kPa (~125 psia) (see Figure 10). This yields a film velocity of 58 m/s and an estimated film thickness of ≤13 μm. Due to several uncertainties, the value of 13 μm should be considered a very rough estimation and may be regarded as an upper bound.

5. Mass transport estimates

Based on these results, the mass transport to the beam line at the opening of the upstream resonator section was calculated using two numerical estimates of the temperature distribution in the Li thin film when exposed to a high-power U beam. In these calculations, the initial charge state of the incident beam, the initial energy of the incident beam, and the beam current were kept constant and taken to be 34+, 17 MeV/u, and 10 particle-μA, respectively to simulate a U beam produced by AEBL. The Li film was 13 μm thick, flowing at 58 m/s; the same values as obtained in the experiment. In the first calculation, the diameter of the beam spot was taken to be 1 mm. In the second calculation, however, the beam diameter was taken to be 3 mm for comparison. LISE for Excel was used to calculate the volumetric heat deposition from the U beam in the film. The calculated value for the volumetric heat deposition was used in a Fortran code to obtain the temperature distribution in the film [8] and the mass transport distribution in the beam line opening. The schematic of the beam line configuration used in these calculations is shown in Figure 12. A third calculation was also performed to provide the baseline mass transport from the Li film with zero beam power deposition. Since the liquid Li has a finite vapor pressure, even when the beam power deposited is zero, the mass transport from the film is not zero.

The mean free path of Li monatomic vapor, L in the beam line is conservatively estimated as 7 m from,

$$L = \frac{kT}{\sqrt{2}\pi d^2 P}\ , \tag{1}$$

where T is the temperature of Li vapor in the beam line, d is the diameter of the Li atom, and P is the Li vapor pressure in the beam line. As a conservative estimate, it was assumed that T =300 K, $d = 364\times10^{-12}$ m (van der Waals diameter) for a Li atom [9], and $P = 10^{-3}$ Pa. Since 7 m is much larger than the physical dimension of the system considered here, for calculating the mass transport distribution, it may be assumed that Li vapor acts as collisionless gas. Therefore, the mass transport mechanism was assumed to be the same as the radiative transport mechanism such that the mass flux from the point 1 on the Li film to the point 2 elsewhere is given as,

$$\phi_2'' dA_2 = \phi_1'' dA_1 \frac{\cos\theta_1 \cos\theta_2}{\pi L_{12}^{\ 2}} dA_2\,, \tag{2}$$

where the symbol ϕ'' is the mass flux density at the surface, dA is a small surface area, θ is the angle between the normal direction of the area and the direction to the other area, and L is the distance between point 1 and 2 (see Figure 13). It must be noted that ϕ_1'' is the mass flux density leaving the point 1 on the film and ϕ_2'' is the mass flux density that originates from the point 1 and arrives at the point 2.

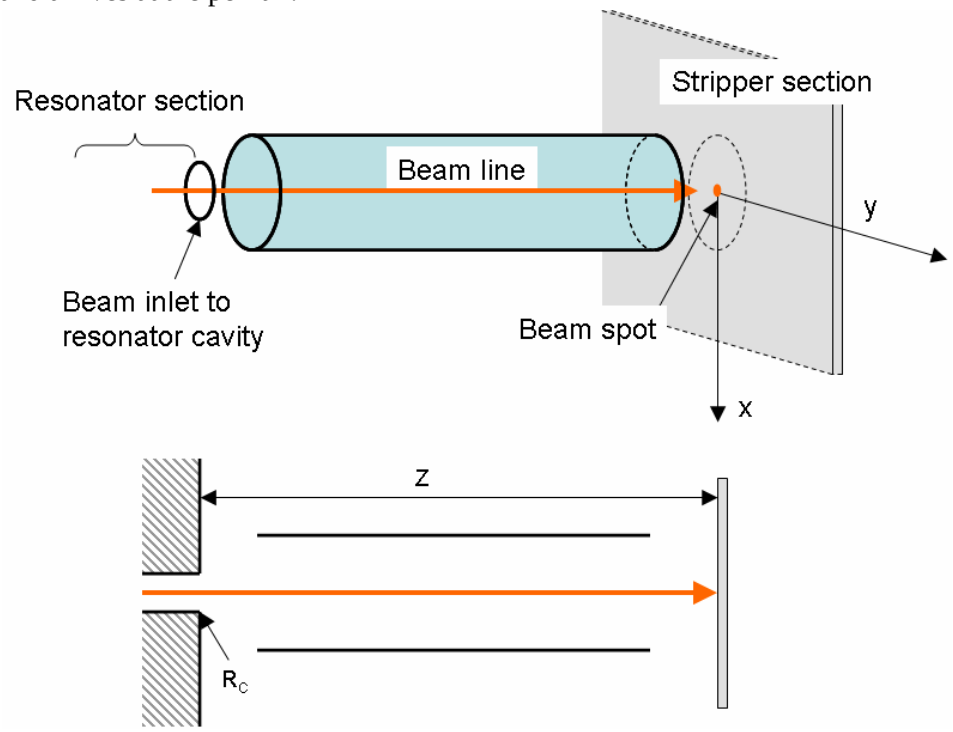

Figure 12. Beam line structures.

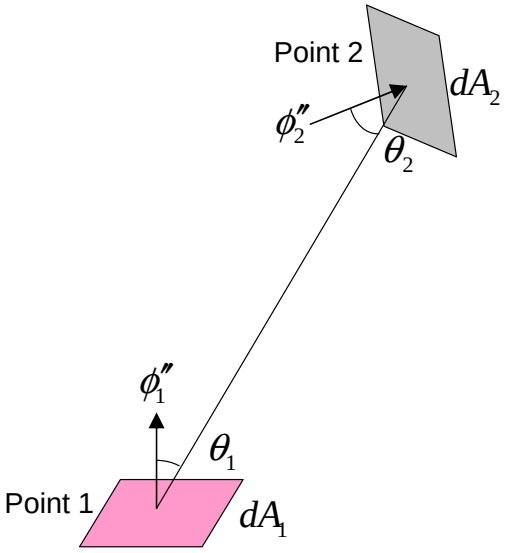

Figure 13. Mass transport view factor.

The assumed beam line configuration is shown in Figure 12. In these example calculations, the distance between the resonator opening and the stripper film, Z, is taken to be 1 m. The resonator cavity opening, R_C, is taken to be 0.025 m. It was assumed that Li vapor intercepted by the beam line structures sticks to the structure and does not contribute to the mass flow to the upstream of the beam line beyond the resonators. The saturation vapor pressure of Li as a function of temperature is given as,

$$P_{SAT} = 10\wedge\left(12.9992 - \frac{8442.53}{T} - 1.64038\times\log_{10}(T) + 2.5968\times10^{-4}\times T\right)\times\frac{10^5}{760.06}, \quad (3)$$

where P_{SAT} is the saturation vapor pressure of Li in Pascal and T is the temperature of Li in Kelvin. The Li mass flux density, ϕ'', from the point source of pressure at P is given as,

$$\phi'' = \frac{1}{4} M_{Li} n_{Li} v_{th}, \quad (4)$$

where M_{Li} is the atomic mass of Li in kg, the number density of Li, n_{Li} is given as,

$$n_{Li} = \frac{P}{kT}, \quad (4)$$

and the mean thermal velocity, v_{th} is given as,

$$v_{th} = \sqrt{\frac{8kT}{\pi M_{Li}}}, \quad (4)$$

where k is the Boltzmann's constant. The actual calculation procedure is described as follows:

1. Calculate the temperature field of the film,
2. Calculate the mass flux density at a point on that is the beam line opening at the resonator,
    a. Calculate the mass flux density using eq. (4) at each point on that is the film surface. The mass flux density is calculated using the temperature at that point obtained in the step 1.
    b. Integrate the RHS of eq. (2) over the film surface. This gives the overall mass flux density at a point on ,
3. Integrate the mass flux density over the resonator opening. This gives the overall mass flux density entering the resonator opening.

The results shown in Table 2 indicate calculated peak temperatures of 941 K and 663 K, which correspond to Li vapor pressures of 33 Pa and 8.5×10^{-3} Pa for 1 mm and 3 mm diameter beams, respectively. Note that Case 3 in the table shows the Li mass transport without beam for comparison. At these conditions, the mass transport to the resonator opening is estimated to be 2.5×10^{-10} kg/s and 1.4×10^{-13} kg/s. These are equivalent to ~8 g and ~4 mg, respectively, per year of full power beam-on-stripper operation. The former is too large considering potential contamination of the beam lines and accelerator. However, for the case of the 3 mm beam spot size, the amount of Li transport is greatly reduced and may not become a serious contamination issue, manifesting the feasibility of the liquid lithium windowless stripper concept with proper optimization of beam line configuration and beam profile. Further reduction of the mass

transport of lithium entering the resonator can be ensured by introducing a small magnetic chicane in the beam line to eliminate line-of-sight transport.

Table 2. Calculated values for Li films interacted with a U beam.

	Case 1	Case 2	Case 3
Thickness (mg/cm^2)	0.66	0.66	0.66
(μm)	13	13	13
Film velocity (m/s)	58	58	58
Beam diameter (= 2×1.41σ, mm)	1	3	NA
Energy loss in film (W)	624	624	0
Volumetric heat deposition (W/m^3)	6.32×10^{13}	7.03×10^{12}	0
Maximum temperature in the film (K)	**941**	**663**	**523**
Maximum Li saturation vapor pressure (Pa)	**33**	**8.5×10^{-3}**	**4.5×10^{-6}**
Total mass transport (kg/s)	**2.5×10^{-10}**	**1.4×10^{-13}**	**9.0×10^{-15}**

6. Summary and conclusions

A high pressure liquid lithium system was constructed which was capable of driving liquid lithium at up to 13.9 MPa (2000 psia) through a nozzle opening as large as 1 mm (40 mil) in diameter. Experiments were performed to demonstrate the formation of a liquid lithium thin film jet that simulates a liquid lithium thin film stripper for AEBL. A thin film of 9 mm in width at velocity of ~58 m/s was formed. Its thickness was estimated to be roughly <~13 μm. However, more work is needed to determine the thickness of the film more accurately. The chamber pressure remained below 10^{-5} Torr during the experiment. Lithium mass transport rates were estimated for various beam diameters. This demonstration gave a preliminary indication of the feasibility of using a liquid lithium thin film stripper for the AEBL driver linac. Further tests are planned to determine short and long term thickness stability and the response of the film to beam power [10, 11]. This type of liquid metal thin film may also find applications in other areas where a high power beam is used, such as high power X-ray source development.

Acknowledgments

The authors would like to thank Robert Haglund of ANL for his technical support. The submitted manuscript has been created by the University of Chicago as Operator of the Argonne National Laboratory under Contract No. DE-AC02-06CH11357 with the U.S. Department of Energy. The U.S. Government retains for itself, and others acting on its behalf, a paid-up, nonexclusive, irrevocable worldwide license in said article to reproduce, prepare derivative works, distribute copies to the public, and perform publicly and display publicly, by or on behalf of the Government.

References

[1] J. A. Nolen, *Plans for an Advanced Exotic Beam facility in the U.S.*, *Nucl. Phys.* **A787** (2007) 84.

[2] J. A. Nolen et al., *Behavior of Liquid Lithium Jet Irradiated by 1 MeV Electron Beams up to 20 kW*, *Rev. Sci. Instrum.* **76** (2005) 073501.

[3] J. P. Rozet, D. Vernhet, and C. Stephan, *ETACHA: A program for calculating charge states at GANIL energies.*, *Nucl. Instrum. Methods* **B107** (1996) 67.

[4] C. Scheidenberger et al., *Charge states of relativistic heavy ions in matter*, *Nucl. Instrum. Methods* **B142** (1998) 441.

[5] A. Leon et al., *Charge State Distributions of Swift Heavy Ions Behind Various Solid Targets (36 ≤Zp≤ 92, 18 MeV/u ≤E≤ 44 MeV/u)*, *At. Data Nucl. Data Tables* **69** (1998) 217.

[6] S. P. Lin and R. D. Reitz, *Drop and Spray Formation from a Liquid Jet*, *Annu. Rev. Fluid Mech.* **30** (1998) 85.

[7] Y. Momozaki, *Research Proposal for Development of an Electron Stripper Using a Thin Liquid Lithium Film for Rare Isotope Accelerator*, *ANL-06/06*, 2006.

[8] Y. Momozaki and J. A. Nolen, *On a Thermal Analysis of a Second Stripper for RIA*, *ANL-06/10*, 2008.

[9] A. Bondi, *van der Waals Volumes and Radii*, *J. Phys. Chem.* **68** (1964) 441.

[10] Y. Momozaki, J. A. Nolen, and C. B. Reed, *Li Thin Film Thickness Measurements Using Low Energy Electron Beam*, in proceedings of *the Eighth International Topical Meeting on Nuclear Applications and Utilization of Accelerators (AccApp '07)*, American Nuclear Society, LaGrange Park, IL, (2007) 100.

[11] S. Kondrashev et al., *Upgrade of the FRIB Prototype Injector for Liquid Lithium Film Testing*, Particle Accelerator Conference (PAC09), May, 4-8, 2009, Vancouver, British Columbia, Canada.